Communication

# Electrocatalysis on Bimetallic Surfaces: Modifying Catalytic Reactivity for Oxygen Reduction by Voltammetric Surface Dealloying

Shirlaine Koh, and Peter Strasser

*J. Am. Chem. Soc.*, **2007**, 129 (42), 12624-12625• DOI: 10.1021/ja0742784 • Publication Date (Web): 02 October 2007

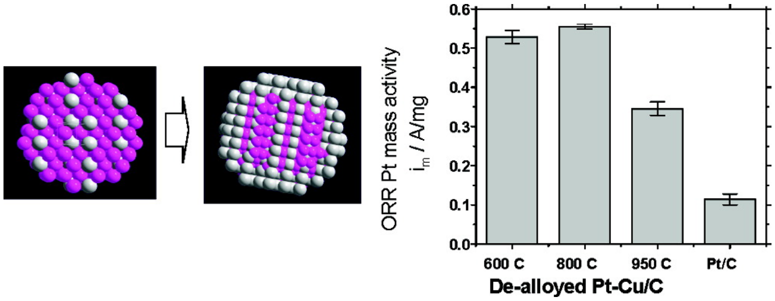

Journal of the American Chemical Society is published by the American Chemical Society. 1155 Sixteenth Street N.W., Washington, DC 20036

J|A|C|S
COMMUNICATIONS

# Electrocatalysis on Bimetallic Surfaces: Modifying Catalytic Reactivity for Oxygen Reduction by Voltammetric Surface Dealloying

Shirlaine Koh and Peter Strasser*

*Department of Chemical and Biomolecular Engineering, University of Houston, Houston, Texas 77204*

Received July 5, 2007; E-mail: pstrasser@uh.edu

The surface electrocatalytic reactivity of noble metals, for instance Pt, has frequently been modified by alloying Pt with less noble metal atoms within the top surface and/or subsurface layer.[1,2] Monolayers of pure Pt deposited on top of non-Pt substrates also showed significantly altered surface catalytic reactivity.[3] Here, we report a distinctly different synthetic strategy to modify the surface reactivity of Pt. The synthesis involves electrochemical surface dealloying, that is, selective electrodissolution, of non-noble metal atoms from bimetallic precursors. In particular, we report on significant activity enhancements for the oxygen reduction reaction (ORR) after Cu dealloying from carbon-supported Pt−Cu alloy nanoparticle electrocatalysts. After removal of Cu atoms from the surface region, the resulting particle catalysts showed previously unachieved 4−6-fold activity improvements over pure Pt.[4] Pt has been the ORR electrocatalyst of choice for decades, yet the search for more active electrocatalysts continues to be a key scientific and technological challenge in the area of electrochemical energy conversion and has become a "conditio sine qua non" in polymer electrolyte membrane fuel cell research.

The electrocatalytic activity of dealloyed Pt−Cu catalysts for the oxygen reduction reaction (ORR) is demonstrated by sweep voltammetric measurements in $O_2$ saturated electrolyte using a rotating disk electrode (Figures 1, 2, and Supporting Information Figure S1). Cyclic voltammetric (CV) characterization of the dealloyed Pt−Cu catalyst surfaces in $O_2$ free electrolyte (inset Figure 1) resembled those of pure Pt, indicating no residual Cu atoms near the surface after dealloying. The CV peak associated with the formation of oxygenated adsorbates (0.8−0.9 V) was shifted to more anodic potentials suggesting the delayed formation of Pt-oxides after dealloying.[2,5] The steep portion of the voltammetric ORR curves (Figure 1) were considerably shifted to higher potentials indicating significant ORR activity (negative reduction current density) at lower overpotentials (higher electrode potentials) compared to pure Pt. Figure 2 shows a quantitative comparison of the Pt-mass based ($A/mg_{Pt}$) (Figure 2a) and the Pt surface-area based ($\mu A/cm^2_{Pt}$) (Figure 2b) activities of the dealloyed Pt−Cu catalysts in the kinetically controlled regime. At 0.9 V the Pt−Cu nanoparticle catalysts outperformed pure Pt by a unprecendented[4] factor of 4−6 times. The catalysts synthesized from a $Pt_{25}Cu_{75}$ precursor that was annealed at 800 °C even exceeded catalyst performance targets of ORR fuel cell catalysts (0.44 $A/mg_{Pt}$ and 720 $\mu A/cm^2_{Pt}$ at 0.9 V) set by the Department of Energy[4] (Figure S1).

The electrochemical surface areas (Figure S1c and Table S1) of the dealloyed $Pt_{25}Cu_{75}$ catalyst showed no significant increase compared to pure Pt, ruling out pure surface area enhancement effects.

The synthesis of the electrocatalyst is a two-step process involving the preparation of carbon-supported Cu-rich precursor alloys (Pt/Cu stoichiometry of 1:3, $Pt_{25}Cu_{75}$) followed by electrochemical dissolution of Cu (dealloying).

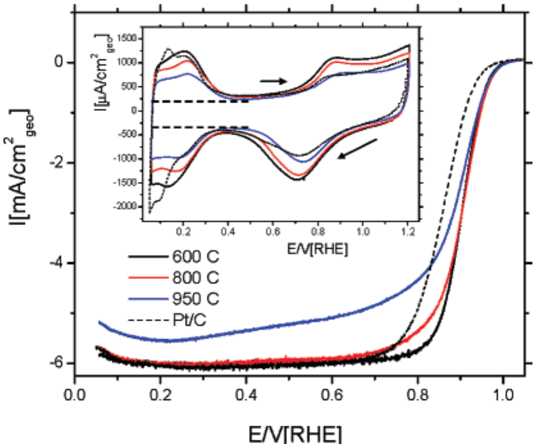

***Figure 1.*** Sweep voltammetry of dealloyed $Pt_{25}Cu_{75}$ catalysts, annealed at 600 °C (black), 800 °C (red), 950 °C (blue), compared to Pt (dotted). The inset shows the cyclic voltammograms of the catalysts in $O_2$ free electrolyte. The horizontal black dotted line indicates the positive and negative capacitance currents. Arrows indicate scan directions.

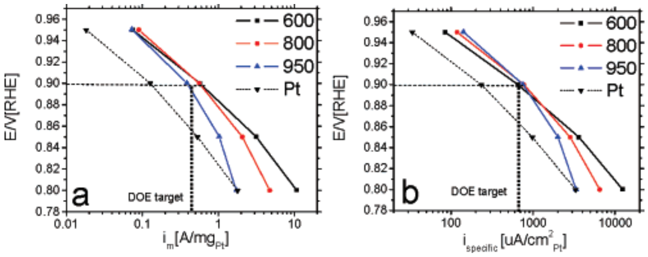

***Figure 2.*** Potential-activity plots of dealloyed $Pt_{25}Cu_{75}$ catalysts compared to pure Pt: (a) Pt mass-based activities; (b) Pt surface area specific activities.

The Cu-rich catalyst precursors were prepared by a conventional impregnation−reductive annealing method. We compare results obtained from three different catalyst precursors annealed at 600, 800, and 950 °C.

Structural characterization of the three precursors was carried out using X-ray diffraction (XRD) (Figure 3).

All three precursor compounds showed reflection profiles consistent with a face-centered cubic (fcc) crystal symmetry. The shift of the strong Pt−Cu(111) reflections (at $2\theta \approx 42°$) to higher angles compared to the pure Pt(111) peak ($2\theta = 39.7°$) indicates that Cu and Pt atoms formed disordered Pt−Cu alloy phases with reduced Pt−Pt interatomic distance. With higher temperatures, the (111) peaks became narrower suggesting larger particles. The 600 and 800 °C precursors showed peaks of an unalloyed pure Cu phase. More detailed XRD peak analysis is presented in Figure S2 and Table S1. Profile analysis revealed that all three precursors consisted of two distinct alloy phases ("fcc1"and "fcc2" in Table S1). The compositional differences between phases fcc1 and fcc2 decreased with temperature. The peak intensity ratio between the alloy peaks and the pure Cu peaks increased with temperature. The peak intensity ratio between the Cu-rich alloy phase fcc 2 and the Pt-

10.1021/ja0742784 CCC: $37.00 © 2007 American Chemical Society

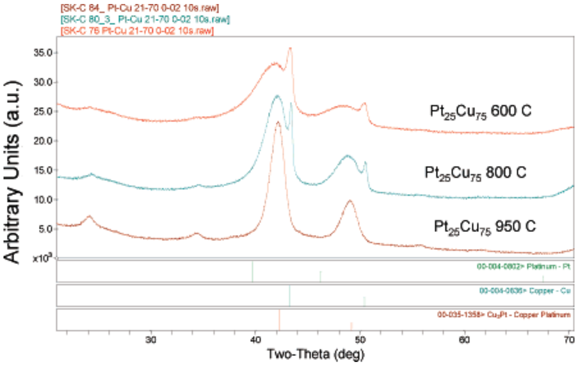

*Figure 3.* X-ray diffraction profiles of carbon-supported $Pt_{25}Cu_{75}$ precursor catalysts annealed at three different temperatures.

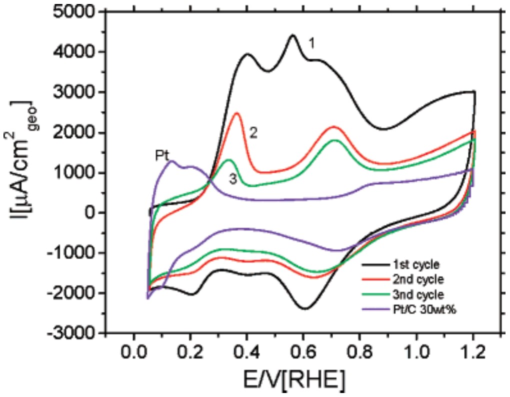

*Figure 4.* Initial three cyclic voltammetric (CV) profiles (1,2,3) of a $Pt_{25}Cu_{75}$ precursor catalyst (annealed at 600 C) during electrochemical dealloying at 100 mV/s. For comparison, the CV of a Pt standard catalyst is shown in blue.

rich alloy fcc 1 increased with temperature. These observations are consistent with a more complete degree of alloying at elevated temperatures.

The selective electrochemical dissolution (dealloying) of Cu is the key process in the formation of the active catalyst. Figure 4 shows the voltammetric characteristics during the initial stage of the dealloying process. The first cycle shows no H-ad/desorption (0.05−0.3 V) consistent with complete Cu surface segregation in Cu-rich Pt alloys.

Sweeping anodically, Cu dissolution peaks appeared at 0.3 V and stretched to 0.85 V. On the second cycle, additional anodic Cu dissolution occurred at two narrower potential regions around 0.3 and 0.7 V. On the third cycle, the Cu dissolution peaks decreased further in intensity, while H ad/desorption features gradually emerged. After about 200 cycles, the dissolution of Cu was absent resulting in a stable Pt-like CV profile (inset of Figure 1).

The broad Cu dissolution features on the first scan are consistent with a superposition of electrodissolution from a Pt−Cu particle ensemble with a range of different Pt/Cu atomic ratios. While dissolution of pure, unalloyed Cu phases occurs near the Cu standard potential (0.34 V), Cu dissolution from Pt−Cu alloys occurs at more positive electrode potentials. Dissolution near 0.6−0.7 V is consistent with stripping Cu layers from pure Pt or Pt-rich alloy substrates.

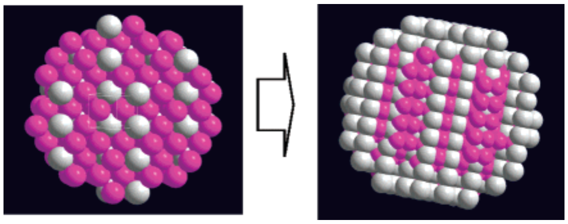

*Figure 5.* Electrochemical dealloying of Cu near the surface of a Cu rich Pt−Cu alloy precursor results in a core−shell particle structure.

To establish a structural and compositional model of the dealloyed Pt−Cu nanoparticles, a comparative bulk (EDX) and surface (XPS) compositional analysis (Table S1 and Figure S4) was performed. The results suggested that at the end of the dealloying process, the $Pt_{25}Cu_{75}$ precursor alloy changed into a substantially Pt enriched Pt−Cu alloy ($Pt_{79}Cu_{21}$) with an essentially pure Pt surface ($Pt_{93}Cu_7$, Figure S4). These finding lead us to hypothesize a core−shell nanoparticle catalyst structure consisting of an essentially pure Pt shell surrounding a Pt−Cu alloy core, as illustrated in Figure 5. Performance stability tests of a dealloyed Pt−Cu catalyst during 4000 potential cycles between 0.6 and 1 V/RHE (Figure S3) indicates that the dealloyed catalyst is able to maintain its activity over longer periods.

As to the mechanistic origin of the activity enhancement in dealloyed Pt−Cu catalyst, our current results point to a key role of geometric effects. This is because the low residual Cu near-surface concentrations make significant electronic interactions between Pt and Cu surface atoms unlikely. Furthermore, selective dissolution of non-noble metals from smooth alloy surfaces can result in increased surface areas[6] (compare Raney catalysts), yet our measured surface areas do not support such a mechanism here for alloy nanoparticles. We therefore suspect that the dealloying creates favorable structural arrangements of Pt atoms at the particle surface, such as more active crystallographic facets or more favorable Pt−Pt interatomic distances[7,8] for the electroreduction of oxygen.

This study demonstrates that electrochemical dealloying of non-noble base metals from base-metal-rich Pt bimetallics significantly alters surface catalytic rates of the resulting Pt shells. The results suggest that surface dealloying may be used as a general synthetic strategy to tune surface catalytic properties of noble metal catalysts for use in heterogeneous gas-phase catalytic or electrocatalytic environments.

**Acknowledgment.** This work was supported by Department of Energy (Lab04-20), TcSUH seed grants; acknowledgment is also made to the donors of the American Chemical Society Petroleum Research Fund for partial support of this research (Grant No. 44165).

**Supporting Information Available:** Additional figures, experimental details, references, tabulated structural, compositional and activity data. This material is available free of charge via the Internet at http://pubs.acs.org.

## References

(1) Stamenkovic, V. R.; Mun, B. S.; Mayrhofer, K. J. J.; Ross, P. N.; Markovic, N. M. *J. Am. Chem. Soc.* **2006**, *128*, 8702.
(2) Stamenkovic, V.; Mun, B. S.; Arenz, M.; Mayerhofer, K. J. J.; Lucas, C. A.; Wang, G.; Ross, P. N.; Markovic, N. *Nat. Mater.* **2007**, *6*, 241.
(3) Zhang, J. L.; Vukmirovic, M. B.; Sasaki, K.; Nilekar, A. U.; Mavrikakis, M.; Adzic, R. R. *J. Am. Chem. Soc.* **2005**, *127*, 12480.
(4) Gasteiger, H. A.; Kocha, S. S.; Sompalli, B.; Wagner, F. T. *Appl. Catal., B* **2005**, *56*, 9.
(5) Stamenkovic, V. R.; Fowler, B.; Mun, B. S.; Wang, G.; Ross, P. N.; Lucas, C. A.; Markovic, N. M. *Science* **2007**, *315*, 493.
(6) Erlebacher, J.; Aziz, M. J.; Karma, A.; Dimitrov, N.; Sieradzki, K. *Nature* **2001**, *410*, 450.
(7) Xu, Y.; Ruban, A. V.; Mavrikakis, M. *J. Am. Chem. Soc.* **2004**, *126*, 4717.
(8) Mavrikakis, M.; Hammer, B.; Nørskov, J. K. *Phys. Rev. Lett.* **1998**, *81*, 2819.

JA0742784